



INSTITUT DE FRANCE
Académie des sciences

Comptes Rendus

Mathématique

Luca Berti, Vincent Chabannes, Laetitia Giraldi and Christophe Prud'homme

Modelling and finite element simulation of multi-sphere swimmers

Volume 359, issue 9 (2021), p. 1119-1127

Published online: 3 November 2021

<https://doi.org/10.5802/crmath.234>



This article is licensed under the
CREATIVE COMMONS ATTRIBUTION 4.0 INTERNATIONAL LICENSE.
<http://creativecommons.org/licenses/by/4.0/>



Les Comptes Rendus. Mathématique sont membres du
Centre Mersenne pour l'édition scientifique ouverte
www.centre-mersenne.org
e-ISSN : 1778-3569



Numerical analysis, Partial differential equations / *Analyse numérique, Equations aux dérivées partielles*

Modelling and finite element simulation of multi-sphere swimmers

Luca Berti^a, Vincent Chabannes^a, Laetitia Giraldi^b
and Christophe Prud'homme^a

^a Cemosis, IRMA UMR 7501, CNRS, Université de Strasbourg, France

^b CALISTO team, INRIA, Université Côte d'Azur, France

E-mails: berti@math.unistra.fr (L. Berti), chabannes@math.unistra.fr (V. Chabannes),
laetitia.giraldi@inria.fr (L. Giraldi), prudhomm@math.unistra.fr (C. Prud'homme)

Abstract. We propose a numerical method for the finite element simulation of micro-swimmers composed of several rigid bodies moving relatively to each other. Three distinct formulations are proposed to impose the relative velocities between the rigid bodies. We validate our model on the three-sphere swimmer, for which analytical results are available.

Résumé. Dans cet article nous proposons une méthode numérique pour la simulation aux éléments finis d'une classe de micro-nageurs. Ces nageurs sont composés par différents corps rigides qui peuvent bouger les uns par rapport aux autres. Nous appliquons notre méthode sur un exemple de micro-nageur connu sous le nom de Three-sphere swimmer.

2020 Mathematics Subject Classification. 65M60, 74F10, 76D07, 76M10.

Manuscript received 7th December 2020, accepted 7th June 2021.

1. Introduction

The dynamics of immersed rigid and deformable bodies in low Reynolds number flows has been extensively studied for its applications to suspension phenomena and the motion of biological micro-organisms [7, 9].

Different numerical methods are used to study these dynamics, such as the Boundary Element method, which discretizes the boundary integral form of Stokes equations [16]; Resistive Force Theory, where the hydrodynamical interactions are approximated by suitable coefficients [1]; the Finite Element method, where the fluid domain is discretized and fitted [11] or unfitted [6] meshes are used for the immersed bodies. In the following, the focus will be on the Finite Element method with body-fitted mesh, where the Arbitrary Lagrangian–Eulerian formalism is used to solve the motion of the fluid domain. The present article is concerned with the simulation of swimmers composed of multiple rigid bodies that move relatively to each other. The advantage of the finite element approach lies on the possibility to generalise the study of swimming micro-organisms beyond the limits presented by other methods [13]. Differently from the finite element

method, analytical descriptions of micro-swimmers are based on asymptotic expansions and are valid in a limited range of the swimmer's parameters; in terms of numerical simulations, the boundary element method hardly generalises to consider complex environments, complex fluids and elastic bodies. The main examples are micro-swimmers composed of spherical bodies, which have been extensively studied via the fundamental solution associated with an immersed rigid sphere [2, 10, 12]. Theoretical and numerical results make these swimmers ideal benchmarking models.

In this paper we propose a numerical method, based on finite elements and the Arbitrary-Lagrangian Eulerian formulation, that allows the simulation of micro-swimmers composed of rigid parts moving relatively to each other, extending [11] to self-propelled swimmers. We illustrate our method by recovering the motion of the three-sphere swimmer, as reported in [12].

2. Mathematical formulation of the problem

In this section we recall the formulation of a generic swimming problem in Stokes flow. Let $\mathcal{F}_0 \subseteq \mathbb{R}^d$, $d = 3$, be the initial configuration of the fluid domain and $\mathcal{A}_t : \mathcal{F}_0 \rightarrow \mathcal{F}_t$ the smooth function that maps the reference fluid domain onto the domain \mathcal{F}_t occupied by the fluid at time t . Let $\mathcal{S}_0 \subseteq \mathbb{R}^d$ be the domain occupied by the swimmer at time $t = 0$ and $\mathcal{S}_t \subseteq \mathbb{R}^d$ be the domain it occupies at time t . Let (u, p) be the fluid velocity and pressure defined over \mathcal{F}_t , μ the viscosity, f the fluid volume forces. We denote by \mathbf{U} and $\boldsymbol{\omega}$ the translational and angular velocities of the swimmer, by x^{CM} its centre of mass and by m and J its volume and geometric inertia tensor. The coupled problem, expressing the kinematic and dynamic coupling of the fluid with the swimmer, reads

$$\left\{ \begin{array}{ll} -\mu\Delta u + \nabla p = f, & \text{in } \mathcal{F}_t, \\ \nabla \cdot u = 0, & \text{in } \mathcal{F}_t, \\ u = \mathbf{U} + \boldsymbol{\omega} \times (x - x^{CM}(t)) + u_d(t, x) \circ \mathcal{A}_t^{-1}, & \text{on } \partial\mathcal{S}_t, \\ m\dot{\mathbf{U}} = -F_{fluid}, \\ J\dot{\boldsymbol{\omega}} = -M_{fluid}. \end{array} \right. \quad (1)$$

where F_{fluid} and M_{fluid} denote the net fluid forces and torques acting on the swimmer. They are computed by integrating the fluid stress and torque on the boundary of the swimmer, where the fluid and solid interact. The function $u_d(t, x)$ denotes the time derivative of body deformation, and it is the driving mechanism of the whole motion, making the otherwise stationary problem time-dependent. In (1), the function $u_d(t, x)$ is a known datum of the problem. It can have an analytical form or come from a numerical model, but in this last case additional equations must be added to (1) in order to describe the generation of $u_d(t, x)$.

The map $\mathcal{A}_t(x)$ is defined as $\mathcal{A}_t(x) = x + \phi_t(x)$, where $\phi_t(x)$ is the solution of the following Laplace problem

$$\left\{ \begin{array}{ll} \nabla \cdot ((1 + \tau)\nabla\phi_t(x)) = 0 & \text{in } \mathcal{F}_0, \\ \dot{\phi}_t(x) = \mathbf{U} + \boldsymbol{\omega} \times (x - x^{CM}(t)) + u_d(t, x), & \text{on } \partial\mathcal{S}_0, \end{array} \right. \quad (2)$$

where τ is a discontinuous function to be specified later.

3. The articulated micro-swimmer

The articulated micro-swimmer is composed of n rigid bodies among which a reference body B_n is identified. This body is linked to all the other bodies B_i , for $i \in \{1 \dots n-1\}$, by arms which are thin and have negligible hydrodynamic effects. The length of these links can be changed via "internal motors" that impose a relative speed between the bodies, leading to self-propulsion.

In principle, each B_i can have a different shape, but we choose to work with spheres for benchmarking purposes. In fact, the motion of some multi-sphere swimmers can be analytically expressed via asymptotic expansions, in the limit of small ratio between the size of the sphere and their distance and small arm oscillations, by using the appropriate Green kernel of Stokes equations [12, 15].

In this section the motion of n independent bodies is first described, by recalling the formulation in [11]. After that, we present the modified formulation that takes into account the relative velocities between the bodies. In the end, we propose three equivalent methods that allow the imposition of the velocity constraints.

3.1. Motion of n independent bodies

Using the same notation as before, the problem of n independent bodies moving in a Stokes fluid reads

$$\begin{cases} -\mu\Delta u + \nabla p = f, & \text{in } \mathcal{F}_t, \\ \nabla \cdot u = 0, & \text{in } \mathcal{F}_t, \\ u = \mathbf{U}_i + \boldsymbol{\omega}_i \times (x - x_i^{CM}(t)), & i = 1 \dots n, \text{ on } \partial B_i, \\ m_i \dot{\mathbf{U}}_i = -F_{fluid}, & i = 1 \dots n, \\ J_i \dot{\boldsymbol{\omega}}_i = -M_{fluid}, & i = 1 \dots n. \end{cases} \quad (3)$$

In this case $u_d(t, x) = 0$, as the bodies move independently of each other and no deformation is present. Hence, $\mathcal{A}_t(x) = x + \phi_t(x)$, where $\phi_t(x)$ is the solution of the Laplace problem

$$\begin{cases} \nabla \cdot ((1 + \tau)\nabla \phi_t(x)) = 0 & \text{in } \mathcal{F}_0, \\ \dot{\phi}_t(x) = \mathbf{U}_i + \boldsymbol{\omega}_i \times (x - x_i^{CM}(t)), & \text{on } \partial B_i, \end{cases} \quad (4)$$

where τ is a piecewise constant coefficient, defined on each element e of the domain's discretization as $\tau|_e = (1 - V_{min}/V_{max})/(V_e/V_{max})$ where V_{max} , V_{min} and V_e are the volumes of the largest, smallest and current element of the domain discretization [8].

In this formulation, the body motion is dictated by fluid stresses only. We now address the variational formulation of (3) and look for a solution $(u, p, \mathbf{U}_i, \boldsymbol{\omega}_i) \in [H^1(\mathcal{F}_t)]^d \times L^2(\mathcal{F}_t) \times [\mathbb{R}^d]^n \times [\mathbb{R}^d]^n$ to the weak formulation of the problem.

Let $(\tilde{u}, \tilde{p}, \tilde{\mathbf{U}}_i, \tilde{\boldsymbol{\omega}}_i) \in [H^1(\mathcal{F}_t)]^d \times L^2(\mathcal{F}_t) \times [\mathbb{R}^d]^n \times [\mathbb{R}^d]^n$ denote the test functions. The variational formulation reads

$$2\mu \int_{\mathcal{F}_t} D(u) : D(\tilde{u}) \, dx - \sum_{i=1}^n \int_{\partial B_i} (-pI + 2\mu D(u)) \tilde{n} \cdot \tilde{u} \, dS - \int_{\mathcal{F}_t} p \nabla \cdot \tilde{u} \, dx = \int_{\mathcal{F}_t} f \cdot \tilde{u} \, dx, \quad (5)$$

$$\int_{\mathcal{F}_t} \tilde{p} \nabla \cdot u \, dx = 0, \quad (6)$$

$$m_i \dot{\mathbf{U}}_i \cdot \tilde{\mathbf{U}}_i = - \int_{\partial B_i} (-pI + 2\mu D(u)) \tilde{n} \cdot \tilde{\mathbf{U}}_i \, dS, \quad i = 1 \dots n, \quad (7)$$

$$J_i \dot{\boldsymbol{\omega}}_i \cdot \tilde{\boldsymbol{\omega}}_i = - \int_{\partial B_i} (-pI + 2\mu D(u)) \tilde{n} \times (x - x_i^{CM}) \cdot \tilde{\boldsymbol{\omega}}_i \, dS, \quad i = 1 \dots n, \quad (8)$$

where $D(u) = \frac{1}{2}(\nabla u + \nabla u^T)$. We remark that the integrals in equations (7) and (8) coincide with F_{fluid} and M_{fluid} respectively. The integration is performed over the boundary of the swimmer as the dynamic continuity is required at the fluid-solid interface of the immersed bodies.

Following [11], we choose $(\tilde{u}, \tilde{\mathbf{U}}_i, \tilde{\boldsymbol{\omega}}_i) \in [H^1(\mathcal{F})]^d \times [\mathbb{R}^d]^n \times [\mathbb{R}^d]^n$ satisfying $\tilde{u} = \tilde{\mathbf{U}}_i + \tilde{\boldsymbol{\omega}}_i \times (x - x_i^{CM})$ on ∂B_i . These test functions form a subspace of $[H^1(\mathcal{F}_t)]^d \times [\mathbb{R}^d]^n \times [\mathbb{R}^d]^n$, and they satisfy the relationship

$$\int_{\partial B_i} (-pI + 2\mu D(u)) \tilde{\mathbf{n}} \cdot \tilde{u} \, dS = \int_{\partial B_i} (-pI + 2\mu D(u)) \tilde{\mathbf{n}} \cdot \tilde{\mathbf{U}}_i \, dS + \int_{\partial B_i} (-pI + 2\mu D(u)) \tilde{\mathbf{n}} \times (x - x_i^{CM}) \cdot \tilde{\boldsymbol{\omega}}_i \, dS, \tag{9}$$

that combines the boundary terms in equations (5)-(7)-(8). The ‘compact’ reformulation

$$2\mu \int_{\mathcal{F}_t} D(u) : D(\tilde{u}) \, dx - \int_{\mathcal{F}_t} p \nabla \cdot \tilde{u} \, dx + \sum_{i=1}^n m_i \mathbf{U}_i \cdot \tilde{\mathbf{U}}_i + J_i \boldsymbol{\omega}_i \cdot \tilde{\boldsymbol{\omega}}_i = \int_{\mathcal{F}_t} f \cdot \tilde{u} \, dx. \tag{10}$$

of equations (5)-(7)-(8) shows that boundary terms have been absorbed by the choice of the finite element spaces.

3.2. The constraints on relative velocities

Among the n bodies composing the articulated swimmer, we identify B_n as the reference body. The velocities \mathbf{U}_i of all the other bodies B_i , $i = 1 \dots n - 1$, are expressed as functions of \mathbf{U}_n via constraints of the form

$$\mathbf{U}_i = \mathbf{U}_n + \mathbf{W}_{in}(t), \quad i = 1 \dots n - 1, \tag{11}$$

where $\mathbf{W}_{in}(t)$ represents the relative velocity between B_i and B_n . The addition of these constraints to (3) completes the formulation of the swimming problem for the articulated swimmers. We notice that the resulting system is a particular instance of the general case presented in (1), where $u_d(t, x)$ is a function of the relative velocities $\mathbf{W}_{in}(t)$ in (11). More precisely, the Dirichlet boundary conditions in (1) would read:

$$\begin{aligned} u &= \mathbf{U}_n + \boldsymbol{\omega}_i \times (x - x_i^{CM}(t)) + \mathbf{W}_{in}(t), & \text{for } i = 1, \dots, n - 1, & \quad \text{on } \partial B_i, \\ u &= \mathbf{U}_n + \boldsymbol{\omega}_n \times (x - x_n^{CM}(t)), & & \quad \text{on } \partial B_n, \end{aligned} \tag{12}$$

which gives $u_d(t, x) = \mathbf{W}_{in}(t)$ for $x \in \partial B_i$, where we define $\mathbf{W}_{nn}(t) = 0$.

The formulation we just described applies directly to the three-sphere swimmer [12], an articulated swimmer composed of three aligned spheres. Here the reference body $B_n = B_3$ is the central sphere, which is connected by extensible arms to the other two spheres B_1 and B_2 . The formulation can be applied as well to the planar three-sphere swimmer [10] or to the four-sphere swimmer [2], whose spherical bodies are placed on the vertices of an equilateral triangle or tetrahedron, respectively. In those cases, the relative velocity vectors \mathbf{W}_{in} should be carefully computed, as each extensible arm connects B_i to the barycentre of the swimmer, and not to B_n directly as in the case of the three-sphere swimmer.

3.3. Discrete and algebraic formulation

Let us consider a geometrical discretization \mathcal{F}_h of the fluid domain using simplexes. The fluid problem is then discretized using an inf-sup stable pair of conforming finite element spaces $X_h(\mathcal{F}_h) \times B_h(\mathcal{F}_h)$ for (u_h, p_h) and $(\mathbf{U}_j, \boldsymbol{\omega}_j) \in [\mathbb{R}^d]^n \times [\mathbb{R}^d]^n$.

Since the fluid velocity satisfies $u = \mathbf{U}_i + \boldsymbol{\omega}_i \times (x - x_i^{CM})$ on ∂B_i , the degrees of freedom $u_{\partial B_i}$ that lie on ∂B_i are treated differently from the remaining ones, that we denote by u_I . Indeed, $u_{\partial B_i}$ are expressed as a function of $(\mathbf{U}_i, \boldsymbol{\omega}_i)$.

At first, equations (5)-(8) are discretized by ignoring the constraint $u = \mathbf{U}_i + \boldsymbol{\omega}_i \times (x - x_i^{CM})$ on ∂B_i . Then, via the operator

$$\mathcal{P} = \begin{bmatrix} I & 0 & 0 & 0 \\ 0 & \tilde{P}_{\mathbf{U}} & \tilde{P}_{\boldsymbol{\omega}} & 0 \\ 0 & I & 0 & 0 \\ 0 & 0 & I & 0 \\ 0 & 0 & 0 & I \end{bmatrix}, \tag{13}$$

that satisfies the equation

$$(u_I, u_{\partial B_i}, \mathbf{U}_i, \boldsymbol{\omega}_i, p)^T = \mathcal{P}(u_I, \mathbf{U}_i, \boldsymbol{\omega}_i, p)^T, \tag{14}$$

the change of finite element basis, from the standard formulation to the constrained one, is performed. In (13), $\tilde{P}_{\mathbf{U}}$ and $\tilde{P}_{\boldsymbol{\omega}}$ contain the interpolation operators that allow to express $u_{\partial B_i}$ as a function of \mathbf{U}_i and $\boldsymbol{\omega}_i$. In particular, if one denotes by D_i the number of velocity degrees of freedom that lie on ∂B_i , one has

$$\tilde{P}_{\mathbf{U}} = \begin{bmatrix} P_{\mathbf{U}_1} & \dots & 0_{D_1 \times d} & \dots & 0_{D_1 \times d} \\ 0_{D_i \times d} & \dots & P_{\mathbf{U}_i} & \dots & 0_{D_i \times d} \\ \dots & \dots & \dots & \dots & \dots \\ 0_{D_n \times d} & \dots & 0_{D_n \times d} & \dots & P_{\mathbf{U}_n} \end{bmatrix} \tag{15}$$

where $P_{\mathbf{U}_i}$ denotes the interpolation operator that expresses the velocity degrees of freedom on ∂B_i as a function of \mathbf{U}_i .

The constraints on the relative velocities between the bodies can be imposed via Lagrange multipliers, through a modification of the operator \mathcal{P} or by modifying the matrix that results from the discretization of the fluid problem.

The first method is the least invasive: additional equations and unknowns are added to a pre-existing discretized problem of n independent bodies in a Stokes fluid, as described in (3). Lagrange multipliers $\alpha_i \in \mathbb{R}^d$, $i = 1 \dots n - 1$ are introduced to impose the constraints on the translational velocities \mathbf{U}_i onto the differential formulation. The previous constraint will appear in the equations that describe the rigid body motion of the solid bodies: equations (7) will be substituted by

$$m_i \dot{\mathbf{U}}_i \cdot \tilde{\mathbf{U}}_i + \alpha_i \cdot \tilde{\mathbf{U}}_i = - \int_{\partial B_i} (-pI + 2\mu D(u)) \tilde{\mathbf{n}} \cdot \tilde{\mathbf{U}}_i \, dS, \quad i = 1 \dots n - 1, \tag{16}$$

$$m_n \dot{\mathbf{U}}_n \cdot \tilde{\mathbf{U}}_n - \sum_{i=1}^{n-1} \alpha_i \cdot \tilde{\mathbf{U}}_n = - \int_{\partial B_n} (-pI + 2\mu D(u)) \tilde{\mathbf{n}} \cdot \tilde{\mathbf{U}}_n \, dS, \tag{17}$$

$$\alpha_i \cdot (\mathbf{U}_i - \mathbf{U}_n) = \alpha_i \cdot \mathbf{W}_{in}, \quad i = 1 \dots n - 1. \tag{18}$$

The addition of Lagrange multipliers entails the modification of \mathcal{P} by providing an additional identity matrix of size $d(n - 1) \times d(n - 1)$ on the diagonal.

Instead of using Lagrange multipliers to constrain the translational velocities, a modification of the operator \mathcal{P} could give the same results. In terms of finite element spaces, this consists in reducing the constrained finite element space to basis functions that satisfy $u = \mathbf{U}_n + \boldsymbol{\omega}_i \times (x - x_i^{CM}(t)) + u_d(t, x)$ on ∂B_i , with $u_d(t, x)$ function of \mathbf{W}_{in} . Equation (14) becomes

$$(u_I, u_{\partial B_i}, \mathbf{U}_i, \boldsymbol{\omega}_i, p)^T = \tilde{\mathcal{P}}(u_I, \mathbf{U}_n, \boldsymbol{\omega}_i, p)^T + u_d, \tag{19}$$

where $\tilde{\mathcal{P}}$ is given by

$$\tilde{\mathcal{P}} = \begin{bmatrix} I & 0 & 0 & 0 \\ 0 & \tilde{\tilde{P}}_{\mathbf{U}} & \tilde{\tilde{P}}_{\boldsymbol{\omega}} & 0 \\ 0 & E & 0 & 0 \\ 0 & 0 & I & 0 \\ 0 & 0 & 0 & I \end{bmatrix}. \tag{20}$$

The $dn \times dn$ block that corresponded to the translational speeds, is presently substituted by the $dn \times d$ matrix

$$\begin{matrix} B_1 \{ \\ \vdots \\ B_i \{ \\ \vdots \\ B_n \{ \end{matrix} \begin{bmatrix} I_d \\ \vdots \\ I_d \\ \vdots \\ I_d \end{bmatrix} = E, \quad (21)$$

and matrix $\tilde{P}_{\mathbf{U}}$ is substituted by

$$\tilde{P}_{\mathbf{U}} = \begin{bmatrix} \tilde{P}_{\mathbf{U}_1} \\ \vdots \\ \tilde{P}_{\mathbf{U}_i} \\ \vdots \\ \tilde{P}_{\mathbf{U}_n} \end{bmatrix}. \quad (22)$$

This modification must be applied directly to the construction of \mathcal{P} , because an a posteriori change of the operator would be too costly in terms of operations on the compactly stored matrix. The relative velocities will then be imposed on the right-hand side of the problem, as the known part of the body velocity.

The last modification is even more invasive, and it consists in modifying the system matrix and right-hand side by substituting (7) with

$$\begin{aligned} (\mathbf{U}_i - \mathbf{U}_n) \cdot \tilde{\mathbf{U}}_i &= \mathbf{W}_{in}(t) \cdot \tilde{\mathbf{U}}_i, & i = 1 \dots n-1, \\ m_n \dot{\mathbf{U}}_n \cdot \tilde{\mathbf{U}}_n &= - \int_{\partial B_n} (-pI + 2\mu D(u)) \vec{n} \cdot \tilde{\mathbf{U}}_n \, dS. \end{aligned} \quad (23)$$

Among the three formulations just presented, we implemented the first two.

The numerical solution of the algebraic system is performed iteratively. The block preconditioning strategy is based on algebraic factorisation and approximation of the Schur complement. The block containing the velocities of the fluid and bodies is block-preconditioned using an incomplete Gauss–Seidel approach, where the fluid velocity is preconditioned via an algebraic multigrid approach and the body velocity block using an LU preconditioning. The pressure block, instead, is preconditioned using the pressure mass matrix [5]. If the Lagrange multiplier formulation is chosen, the Lagrange multipliers are assigned to the body velocity block and preconditioned analogously.

Table 1 presents the algebraic solution strategy and runtime per time iteration for the simulation of a three-sphere swimmer on 8 cores. It is shown that block preconditioning (fieldsplit) leads to faster solution and that the formulation based on $\tilde{\mathcal{P}}$ is slightly more efficient than the approach based on Lagrange multipliers as the mesh is refined. Block preconditioners are built using PETSc fieldsplit, and a comparison is performed with MUMPS LU preconditioning and PETSc $\text{gasm}+LU$ preconditioners based on Additive Schwarz domain decomposition with LU preconditioning on the sub-domains. We note that the $\text{gasm}+LU$ preconditioner fails on the Lagrange Multiplier formulation while LU becomes very expensive as we refine the mesh. The results show that it is necessary to have a solution strategy as generic strategies are not scaling well (or not at all) either in iteration count or computing time. Our solution strategy, based on block preconditioning, is almost optimal in the sense that the number of iterations increases only slightly as the number of unknowns increases.

Table 1. Numerical study on the algebraic solution of the three-sphere swimmer problem. The simulation was launched on 8 cores, and “Time” is the runtime for one time iteration. For the three meshes, the average element size is 3, 2 and 1.5 respectively. For the second and third mesh, in parentheses, we reported the ratio of degrees of freedom, number of iterations and time with respect to the first mesh.

Degrees of freedom ($u + p$)	Formulation	Preconditioner	N. iterations	Time
311000	Lagrange multipliers	LU	-	190s
311000	Lagrange multipliers	fieldsplit	41	33s
311000	Lagrange multipliers	gasm+LU	-	∞
311000	Matrix $\tilde{\mathcal{P}}$	LU	-	190s
311000	Matrix $\tilde{\mathcal{P}}$	fieldsplit	36	30s
311000	Matrix $\tilde{\mathcal{P}}$	gasm+LU	170	80s
888000 (2.85)	Lagrange multipliers	fieldsplit	50 (1.22)	110s (3.33)
888000 (2.85)	Lagrange multipliers	gasm+LU	-	∞
888000 (2.85)	Matrix $\tilde{\mathcal{P}}$	fieldsplit	43 (1.19)	97s (3.23)
888000 (2.85)	Matrix $\tilde{\mathcal{P}}$	gasm+LU	350(2.06)	505s (6.31)
2094000 (6.73)	Lagrange multipliers	fieldsplit	66 (1.60)	350s (10.6)
2094000 (6.73)	Lagrange multipliers	gasm+LU	-	∞
2094000 (6.73)	Matrix $\tilde{\mathcal{P}}$	fieldsplit	53 (1.47)	293s (9.76)
2094000 (6.73)	Matrix $\tilde{\mathcal{P}}$	gasm+LU	395(2.32)	2550s (31.87)

4. The three-sphere micro-swimmer

The three-sphere micro-swimmer [12] is a three-dimensional swimmer composed of three aligned spheres having the same radius R . The two outer spheres are connected to the central one by extensible links, and the propulsion of the swimmer is ensured by changing the lengths of the connecting arms between two fixed values. The arm shrinkage is performed in a non-reversible fashion, in order to break the time-reversal symmetry of the Stokes equations, with a constant relative speed between the central sphere and the approaching one. For example, if the left arm is shrinking and the right arm keeps its length fixed, the translational speed \mathbf{U}_3 and \mathbf{U}_2 of the central and right sphere coincide, while the speed of the left sphere, moving with relative speed \mathbf{W}_{13} with respect to the centre sphere, will be $\mathbf{U}_3 + \mathbf{W}_{13}$. The (non-reciprocal) stroke is composed of 4 steps, as shown in Figure 1, where the lengths of the two arms are alternatively modified.

A quantitative example of swimming is presented in [12]: if $L = 10R$ is the length of each link in its rest position and $a = 4R$ is the maximal variation for the length of each arm (leaving a link length of $6R$ when the arms are completely shrunk), the centre sphere is displaced by $0.16R$ in the positive direction at the end of the 4-step stroke. In the first step, the travelled distance is $1.35R$ in the negative direction; in the second step, it is $1.44R$ in the positive direction; in the third step, it is $1.44R$ in the positive direction; in the fourth step, it is $1.35R$ in the negative direction.

Using the aforementioned Lagrange multipliers formulation, we are able to recover the displacement at each step of the 4-step stroke reported in [12]. Figure 2, on the left, translates the steps of the body deformation in terms of relative velocities between the central and lateral spheres. Figure 2, on the right, represents the motion of B_3 during several repetitions of the 4-step stroke.

The results were obtained using the library FEEL++ [3] and in particular its toolbox for the solution of Navier–Stokes equations in moving domains including moving rigid bodies. The implementations of Lagrange multiplier and \mathcal{P} modification formulations are available in FEEL++ GitHub repository [4] and can be used to reproduce the results in sequential and parallel. The

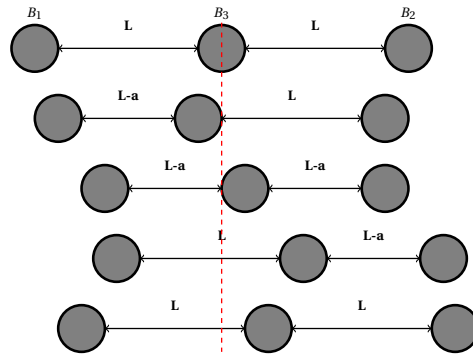


Figure 1. Representation of the three-sphere swimmer and its swimming gait. The gait is composed of four strokes in which one of the arms is alternatively shrunk or elongated. The alternation guarantees the non-reciprocity of the motion.

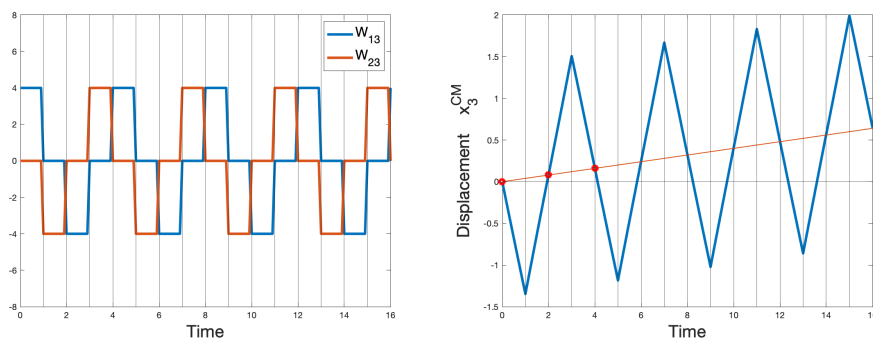


Figure 2. The left figure presents the relative speed W_{13} , between the central and left sphere, and the relative speed W_{23} , between the central and right sphere, as functions of time. The right figure shows, in blue, the position of the central sphere during the 4-step stroke. The red line intersects the trajectory of the central sphere at the red circles, which mark the $0.08R$ and $0.16R$ displacements predicted in [12] after 2 and 4 steps composing the swimming stroke.

computational domain was discretized using a variable element size, finer on the surface of the spheres, generating a total number of 13500 nodes and 78000 tetrahedra. During the simulation, the mesh quality degrades but this does not stop the simulation or affect the results we obtain. The mesh adaptation is performed with a variation of the Laplacian smoothing [8], as a piecewise constant coefficient, depending on the size of the element, is designed to mainly deform larger tetrahedra as opposed to smaller ones. The boundaries of the fluid domain were sufficiently far from the three-sphere swimmer in order compare our results to the analytical ones. However, we remark that the interest of the finite element approach is that the geometry of the fluid domain can be easily modified and the effects of boundaries on the motion of the swimmer can be studied.

5. Conclusion

In this paper, we provide a numerical method to simulate a self-propelled micro-swimmer composed of rigid bodies. Different formulations are proposed, including one based on Lagrange

multipliers, to impose the relative motion between its components. The correctness of our formulations is verified on the three-sphere micro-swimmer by comparing the displacements obtained numerically to the ones in [12], even if only the results based on Lagrange multipliers are presented here. The numerical method that was proposed can be applied to study the effects that complex environments (obstacles, boundaries) have on the swimming of micro-organisms. Also, it can be used as a basis to study gait optimization via machine learning methods to improve propulsion, similarly to [14], or to escape the attractive effects that originate from the interaction with solid boundaries. Current work includes the treatment of other multi-body swimmers like the planar 3-sphere swimmer [10] or the 4-sphere swimmer [2], formulating the ALE framework with mesh adaptation, the extension to other fluid models, e.g. Navier–Stokes and non-Newtonian, and the coupling with elasticity models to handle deformable bodies, i.e. swimmers.

References

- [1] F. Alouges, A. DeSimone, L. Giraldi, M. Zoppello, “Self-propulsion of slender micro-swimmers by curvature control: N-link swimmers”, *Int. J. Non-Linear Mech.* **56** (2013), p. 132-141.
- [2] F. Alouges, A. DeSimone, L. Heltai, A. Lefebvre-Lepot, B. Merlet, “Optimally swimming stokesian robots”, *Discrete Contin. Dyn. Syst., Ser. B* **18** (2013), no. 5, p. 1189-1215.
- [3] V. Chabannes, G. Pena, C. Prud'homme, “High-order fluid-structure interaction in 2D and 3D application to blood flow in arteries”, *J. Comput. Appl. Math.* **246** (2013), p. 1-9, Fifth International Conference on Advanced Computational Methods in Engineering (ACOMEN 2011).
- [4] V. Chabannes, C. Prud'homme, “Github Feel++ repository”, https://github.com/feelpp/feelpp/tree/develop/toolboxes/fluid/moving_body/three_sphere.
- [5] H. C. Elman, D. J. Silvester, A. J. Wathen, *Finite Elements and Fast Iterative Solvers: With Applications in Incompressible Fluid Dynamics*, Numerical Mathematics and Scientific Computation, Oxford University Press, 2014.
- [6] R. Glowinski, T.-W. Pan, T. I. Hesla, D. D. Joseph, “A distributed Lagrange multiplier/fictitious domain method for particulate flows”, *Int. J. Multiphase Flow* **25** (1999), no. 5, p. 755-794.
- [7] J. Happel, H. Brenner, *Low Reynolds number hydrodynamics*, Mechanics of Fluids and Transport Processes, Springer, 1983.
- [8] H. Kanchi, A. Masud, “A 3D adaptive mesh moving scheme”, *Int. J. Numer. Methods Fluids* **54** (2007), no. 6-8, p. 923-944.
- [9] S. Kim, S. J. Karrila, *Microhydrodynamics: Principles and Selected Applications*, Butterworth–Heinemann series in chemical engineering, Dover Publications, 2005.
- [10] A. Lefebvre-Lepot, B. Merlet, “A stokesian submarine”, *ESAIM, Proc.* **28** (2009), p. 150-161.
- [11] B. Maury, “Direct simulations of 2D fluid-particle flows in biperiodic domains”, *J. Comput. Phys.* **156** (1999), no. 2, p. 325-351.
- [12] A. Najafi, R. Golestanian, “Simple swimmer at low Reynolds number: Three linked spheres”, *Phys. Rev. E* **69** (2004), p. 062901.
- [13] C. Rorai, M. Zaitsev, S. Karabasov, “On the limitations of some popular numerical models of flagellated microswimmers: importance of long-range forces and flagellum waveform”, *R. Soc. open sci.* **6** (2019), no. 1, p. 180745.
- [14] A. C. H. Tsang, P. W. Tong, S. Nallan, O. S. Pak, “Self-learning how to swim at low Reynolds number”, *Phys. Rev. Fluids* **5** (2020), no. 7, p. 074101.
- [15] V. A. Vladimirov, “On the self-propulsion of an N -sphere micro-robot”, *J. Fluid Mech.* **716** (2013), article no. R1 (11 pages).
- [16] B. J. Walker, R. J. Wheeler, K. Ishimoto, E. A. Gaffney, “Boundary behaviours of *Leishmania mexicana*: A hydrodynamic simulation study”, *J. Theor. Biol.* **462** (2019), p. 311-320.